High Reliability and High Performance of 9xx nm Single Emitter Laser Diodes

L. Bao*, P. Leisher, J. Wang, M. DeVito, D. Xu, M. Grimshaw, W. Dong, X. Guan, S. Zhang, C. Bai, J. G. Bai, D. Wise, R. Martinsen

*n*Light Corporation
Vancouver, WA 98665

ABSTRACT

Improved performance and reliability of 9xx nm single emitter laser diodes are presented. To date, over 15,000 hours of accelerated multi-cell lifetest reliability data has been collected, with drive currents from 14A to 18A and junction temperatures ranging from 60°C to 110°C. Out of 208 devices, 14 failures have been observed so far. Using established accelerated lifetest analysis techniques, the effects of temperature and power acceleration are assessed. The Mean Time to Failure (MTTF) is determined to be >30 years, for use condition 10W and junction temperature 353K (80°C), with 90% statistical confidence.

Key words: Reliability, lifetime, high power lasers, semiconductor laser diodes, multi-cell lifetest, failure mode, 976 nm, 915 nm, MTTF

1. INTRODUCTION

Recently, there is an increasing interest in 9xx nm high brightness fiber-coupled diode laser modules, for both fiber laser pumping and direct use applications. Comparing to bar-based designs, single-emitter-based fiber-coupled diode laser modules offer increased brightness and optical power density [1]. Improved power scaling of fiber-coupled single-emitter-based diode laser modules is closely related to the recent progress in the performance and reliability of high-power broad-area single emitter diode lasers operating in the 9xx nm wavelength band. These improvements have been enabled by advances in the design, epitaxial growth, facet passivation, and packaging of such devices [2-5].

Industrial applications usually require devices to operate at telecom level reliability, with the cumulative device failure rate for two-year operation being less than 2%. Because of the inherent high reliability of these devices, accelerated lifetesting is required to achieve a sufficient number of failures in a reasonable time period. In order to determine the reliability of the device at some rated use level, multi-cell lifetesting, which investigates the reliability of devices operating at several stress levels, must be performed. Reports on multi-cell lifetesting results for high power diode lasers have been somewhat limited [6-12]; fewer yet have reported acceleration models. Further, the statistical error around the obtained acceleration factors has not been reported. This paper expands on results which were originally reported last year [2]; lifetesting has continued over the past year, and sufficient data has been obtained to begin a statistical investigation of the acceleration models describing the reliability of our high-power broad-area lasers operating in the 9xx nm wavelength range. Over 15,000 hours per device has been accumulated (totaling over 2.7 million raw device hours collected), with drive currents from 14A to 18A and junction temperatures from 60°C to 110°C for 95μm stripe, 3.8mm cavity length 9xx nm devices. The failure rates are still very low – only 14 devices total have failed, with 3 of the 7 tested conditions still showing 0 failures by 15000 hours.

* Phone: 360.566.4460 Email: ling.bao@nlight.net

2. HIGH PERFORMANCE AND HIGH RELIABILITY

The design of our 9xx nm broad area diode laser has focused on these main attributes: power/efficiency, reliability, beam divergence and temperature performance. The vertical laser waveguide is selected to be a large optical cavity to reduce the power density load on the facets, for both reliability and beam divergence consideration. The composition and doping concentration in each layer was optimized for both voltage/efficiency and temperature performance. The epitaxial structure is grown by Metal-Organic Chemical Vapor Deposition, with controlled thickness/composition/wavelength in each run and from run to run. The wafers follow a standard fabrication procedure which includes metal contact deposition, isolation, passivation, and coating. Coated bars are cleaved into single emitter chips, and bonded p-side down with AuSn solder onto expansion-matched heatsinks. The devices are subjected to multiple inspection processes, plus a test, burn-in, and test screening. Calibration of measured power and efficiency is NIST-traceable, and all reported values are directly measured from the devices (i.e. effects such as package resistance are not subtracted).

2.1 Performance Summary

The device geometry for the results reported herein consists of a 3.8 mm cavity length with a 95 µm stripe width. The typical optical power and wall-plug efficiency verses continuous wave (CW) drive current for emitters operating at 915 nm and 976 nm are shown in Figure 1. Each plot includes data from 10 devices at a heatsink temperature of 25°C. Threshold current is ~0.5A and slope efficiency at the linear regime of power-current is ~1.1W/A. With optimized electrical and optical designs, these devices demonstrate wallplug efficiencies (at a 10W rated use condition) of ~64% (at 915 nm) and ~67% (at 976 nm). A histogram of peak efficiency for over 2500 devices at 976 nm manufactured over a 6-month period is shown in Figure 2. Over 95% of devices produced demonstrate peak efficiency of 66% or higher. The efficiency performance of devices operating at 915nm is similar.

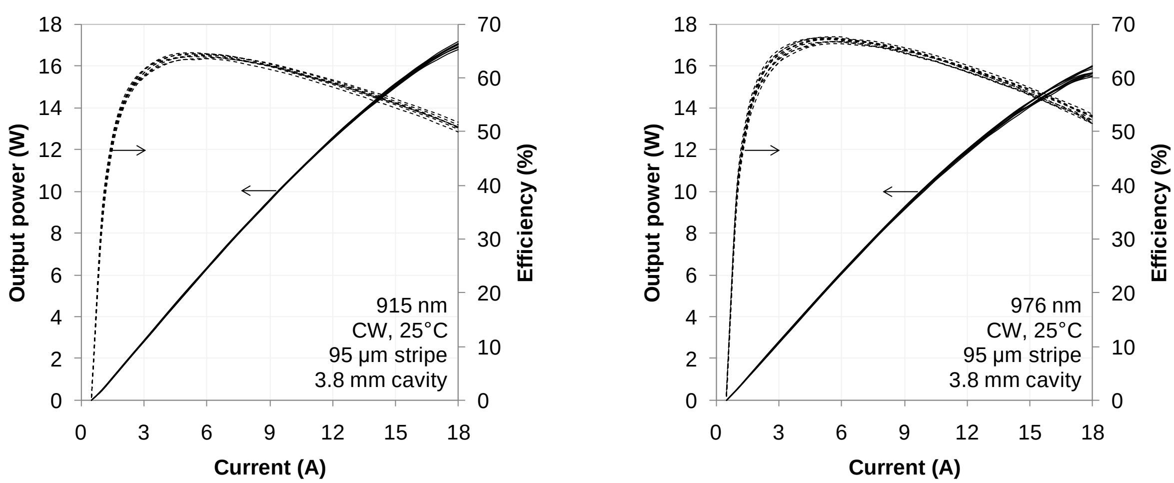

(a) (b)

Figure 1: Typical continuous wave (CW) optical power and wall-plug efficiency verses drive current for ten (a) 915 nm and (b) 976 nm laser diodes operating at 25°C (heatsink).

The 9xx nm design targets a fast axis far-field (FF) full-width half-maximum (FWHM) of around 29° and full-width $1/e^2$ maximum ($FW1/e^2$) of around 49°. Typical slow-axis (SA) divergence measured over various drive currents are shown in Figure 3(a). At 10A operation current, the typical SA FF FWHM is ~ 8.3° and $FW1/e^2$ is around 10.3°. The lateral near field (NF) plots as a function of drive current is shown in Figure 3(b). At 10A operation current, NF $FW1/e^2$ is ~105um. The lateral NF FWHM width is observed to vary slightly with increasing current. On the other hand, the slow axis FF $FW1/e^2$ width increases relatively quickly with drive current. Nevertheless, SA $FW1/e^2$ is only ~10° at 10A operation.

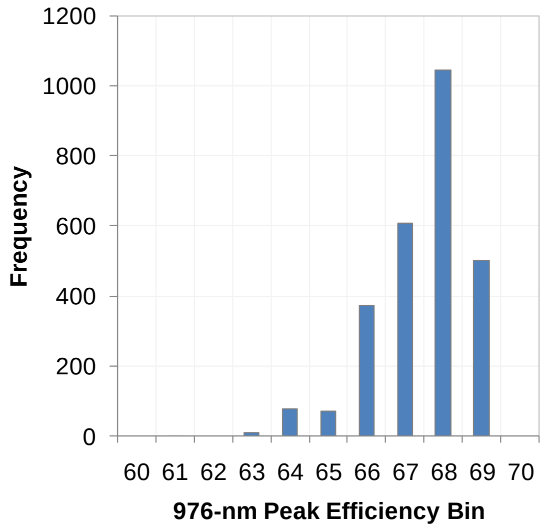

Figure 2: Histogram of peak wallplug efficiency for devices at 976 nm produced over a 6-month period.

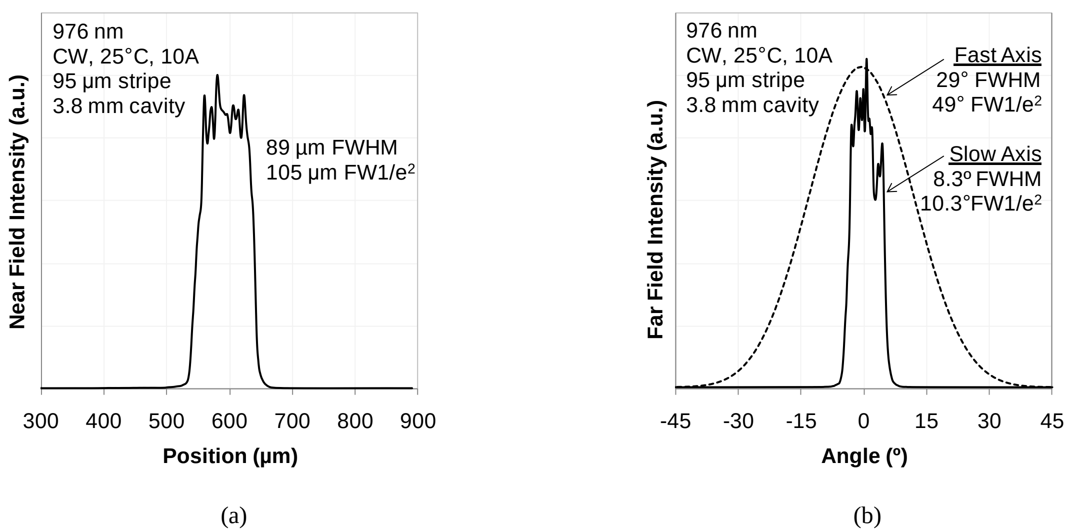

Figure 3: Typical (a) Near-field and (b) far-field intensity measurements of the 976 nm laser design. The results are measured at a 10A operating current, 25°C (heatsink)

2.2 Multi-cell Accelerated Lifetest

For industrial applications, laser failure rate must be sufficiently low to meet customer demands. In many cases, customer reliability requirements may exceed many 10's of thousands of hours. Because reliability requirements are typically many times that of the desirable product development time period, lifetesting at the rated use condition is not practical. Instead, accelerated lifetesting is typically employed to determine device reliability sooner. nLight's general approach to reliability qualification is as follows:

1. A small (~20 devices) lifetest is initiated with the express purpose of providing a preliminary estimate of the reliability and determine the maximum practical operating conditions for the lifetest. Every few hundred hours, the operating conditions are stepped. This test proceeds until most chips have failed.
2. The results of the step-stress test are used to optimize the design of the multicell. A Monte Carlo modeling approach is used to optimize the stress conditions and relative binning of chips into the various cells. This is done in an effort to reduce the relative statistical error vs. test time. In this case, a 7-level multicell test was implemented.
3. Lifetesting results are periodically analyzed. Devices which have not yet failed are treated as suspensions (to the time of analysis) and failure times for failed devices are assessed. The failure statistics dictate the distribution selected for analysis. The data is evaluated in a way which provides both the reliability and acceleration model factors of the test; statistical error for all terms is assessed. The analysis approach is further discussed in 2.3.

Results from nLight's 9xx nm single-emitter multicell lifetest were originally reported last year [2]. At the time, an insufficient # of failures was collected to allow prediction of the acceleration models and reliability with a high degree of accuracy. This lifetest has since continued, bringing the total number of raw device hours to over 2.7 million. The additional failures collected over the past year have helped reduce the statistical error in the previously reported values.

The seven-level can be broken down into two subgroups. One subgroup has four current levels: 12A, 14A, 16A, and 18A, while junction temperature was fixed at 80°C (353K). The other subgroup has four junction temperature levels, 64°C, 80°C, 95°C and 110 °C, while the product of current and power was kept at ~186 AW. To date, the devices on lifetest have each accumulated ~15,000 total hours of operation time, as summarized in Table 1. There are 10 failures from a sum of 166 976 nm lasers, and 4 failures from a total of 42 915 nm lasers.

Multi-cell 7-level lifetest						976nm		915nm	
Lifetest Group	P(W)	I (A)	P*I	Junction T (°C)	Heatsink T (°C)	Units	Failure	Units	Failure
1	15.9	18.0		80	52	10	1	2	2
2	11.3	12.0		80	62	40	2	10	0
3	14.6	16.0		80	55	18	2	6	0
4	13.0	14.0	182	80	58	21	0	3	0
5	11.9	15.7	186	110	88	12	4	3	2
6	12.6	15.0	189	95	73	18	1	6	0
7	13.6	13.7	187	64	42	47	0	12	0
Total						166	10	42	4

Table 1: 7-level multi-cell lifetest design and results

The lifetest curves at 7 levels are shown in Figure 4 (a) and (b), for both 915 nm and 976 nm separately. For the 976 nm lasers, there is no evidence of power degradation in all 7 lifetest groups. The data also did not show any degradation for the 915 nm groups with junction temperatures between 64°C and 80°C. But we did observed for the first time, slow power degradation of 915 nm lasers from the two highest junction temperature levels (lifetest group #6 with 95°C junction temperature and lifetest group #5 with 110°C junction temperature). These 915 nm diode lasers have shown ~10% power degradation in lifetest group #5 (junction T = 110°C). The degradation is confirmed in retest, and is caused by a ~60% increase in threshold current and 10% decrease on slope efficiency by the end of 10,000 hours. There is also ~3% degradation in lifetest group #6 (junction T = 95°C), as measured during a retest at 10,000 hours.

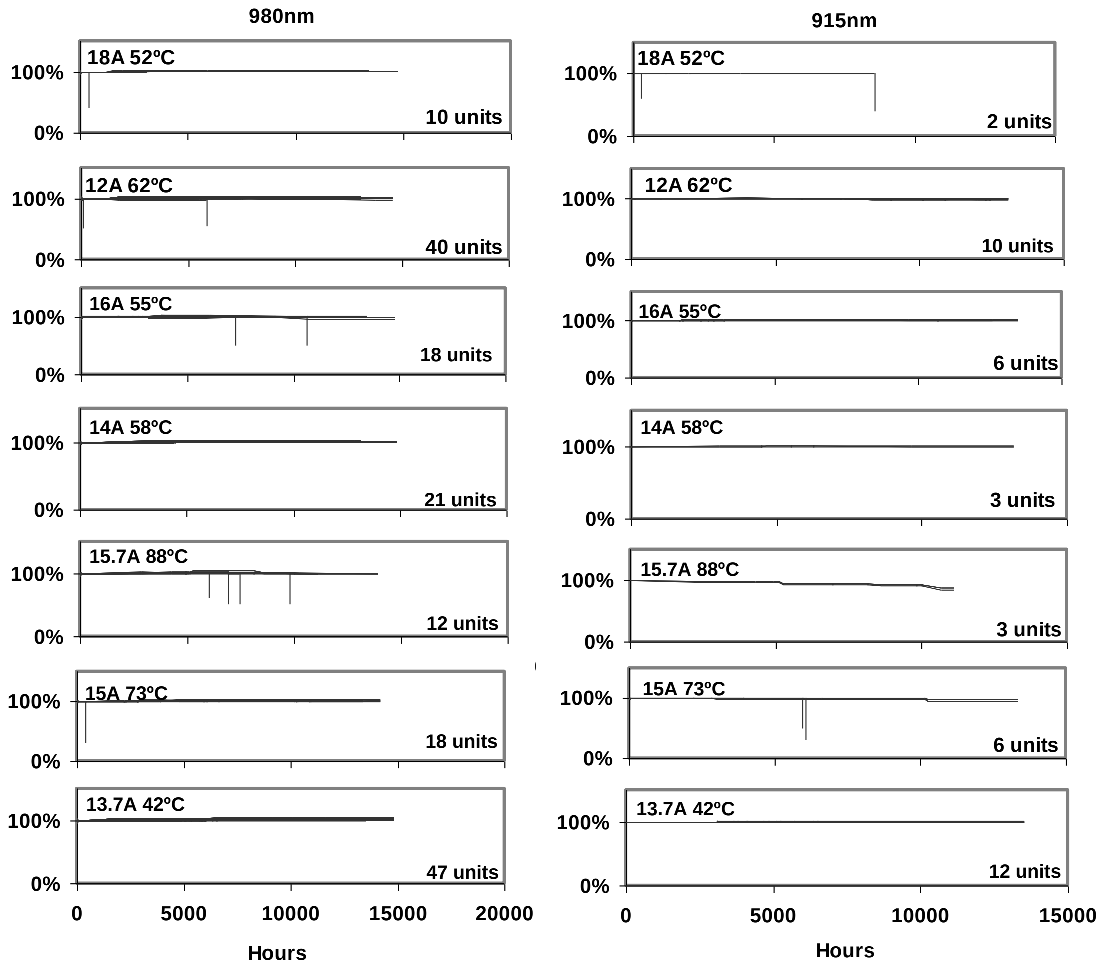

(a) (b)

Figure 4: Multi-cell lifetest plots and failures of (a) 976 nm laser diodes (b) 915 nm laser diodes. Y-axis is normalized power. From top to bottom, the subplots are multi-cell groups 1-7 as in Table 1

Slow degradation is typically believed to be a result of the nonradiative recombination current increase due to Recombination Enhanced Defect Generation (REDG), which has been found accelerated by thermal effect [9, 14]. The physical mechanism of 915 nm slow degradation has not yet been investigated, but it is important to note with respect to the reliability analysis.

2.3 FAILURE ANALYSIS

The method of failure for the 14 observed failures are summarized in Table 2, along with their lifetest conditions and times-to-failure. Several failure analysis techniques [2] have been used to understand the failure mechanisms, including optical microscopy, electrical-luminescence (EL) imaging, photoluminescence (PL) microscope imaging, thermal imaging, SEM, EDX, SIMS and Auger analysis.

Lifetest Group	Current (A)	Heatsink Temp. (°C)	Wavelength (nm)	Failure Type	Failure Time (hours)
1	18A	52	915	COMD	260
1	18A	52	976	BCOD	415
1	18A	52	915	COMD	8560
2	12A	62	976	BCOD	120
2	12A	62	976	BCOD	5890
3	16A	55	976	BCOD	7290
3	16A	56	976	COMD	10630
5	15.7A	88	976	COMD	6000
5	15.7A	88	976	BCOD	6930
5	15.7A	88	976	COMD	7470
5	15.7A	88	976	BCOD	9820
6	15A	74	976	COMD	408
6	15A	73	915	COMD	5940
6	15A	73	915	COMD	6050

Table 2: Laser failures in multi-cell lifetest

The main failure mode found in the 915 nm lasers is Catastrophic Optical Mirror Damage (COMD). To date, all four observed failures in the 915 nm subset are believed to be due to COMD, as evidenced by clear damage to the front laser facet. On the other hand, the 976 nm laser failures have shown a mix of COMD and Bulk Catastrophic Optical Damage (BCOD). Out of the ten observed failures in this subgroup, six are confirmed to have been caused by BCOD, and the remaining four failures are believed to be due to COMD. The reason that COMD cannot be completely confirmed, even in the event of the observation of melt line extending from the facet, is that BCOD events may occasional spread to the facet, resulting in residual damage. This is depicted clearly in n-window imagine experiments previously performed by nLight on 1.5mm cavity length chips, as shown in Figure 5. In this case, the Bulk COD imitates near the center of the laser cavity, and over time, that melt lines are shown to propagate (and even converge on) the front laser facet. Thus the observation of COD melt at the facet is a necessary, but not sufficient, condition to diagnose failure due to COMD. On the other hand, devices which show no melting at the facet, but internal failures can be confirmed to be bulk-initiated COD events.

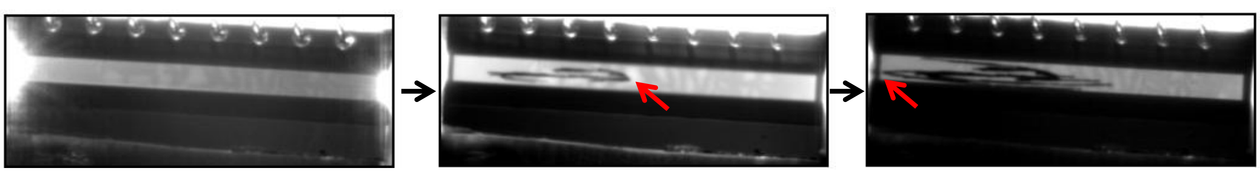

Figure 5: n-window imaging shows that a bulk-initiated COD event can propagate to the facet. If the interim microscope image had not been captured, this device would have (incorrectly) been classified as “COMD.”

The origin of BCOD is still not well understood. Several possibilities include epi-grown defect or a process-induced defect during manufacturing process or handling. In these cases, the failure mode would be expected to present as infant mortality – as the weaker emitters (which contain such defects) would fall out early, leaving behind only “defect-free” devices over the long term. In the case of the 976 nm chips, it seems to be that the BCOD failures occur early in the lifetest, whereas the COMD failures occur later in the lifetest. However, it is not clear if a sufficient number of failures have been gathered to confirm the statistical validity of the result.

2.4 RELIABILITY ANALYSIS

One of the main advantages to perform a multi-cell lifetest with multiple accelerated stress levels is to verify the device failure statistics while simultaneously extracting the acceleration parameters. These acceleration parameters can then be used to predict device reliability under various operating conditions. There are limited data on the acceleration parameters and activation energy from literature, especially for state-of-the-art high power diode lasers. Further, there is no reason to believe that devices produced by different vendors, fabricated in different ways, tested under different conditions, and operating at different wavelengths would necessarily behave in the same fashion under accelerated endurance testing.

The acceleration model which is typically assumed for power and temperature acceleration is a combination of a power law (which describes the effective acceleration due to increasing the operating power of the laser) and the Arrhenius law (which describes the effective acceleration due to increasing the operating temperature of the laser). Equation (1) provides the acceleration of unreliability as a function of power and junction temperature, P is power, T_j is junction temperature, n is the acceleration parameter of power, E_a is the activation energy and k_B is Boltzmann's constant.

$$\text{Acceleration Factor} \propto P^n \exp\left(\frac{-E_a}{k_B \cdot T_J}\right) \tag{1}$$

For high power semiconductor lasers, reported values of E_a span 0.41 eV to 0.64 eV and for n span 2.2 to 5.9 [8-12]. These reported values suffer from being based on very limited experimental trial, device numbers, device failures, lifetest duration and type of devices. To the best of our knowledge, there have been no reports of the statistical uncertainty in these values for high power diode lasers. In this work, we are able to derive for the first time such uncertainties. As we will show, despite a specific effort to optimize the lifetest to determine these values, and the collection of >2.7M raw device hours, the uncertainty in these factors is very large.

First, each multi-cell lifetest group is separately analyzed with Weibull distribution fitting. The shape factor β is then obtained with 90% statistical confidence ranges. Figure 6 is the plot showing the shape factor β for each multi-cell group 1-7 as in Table 1. As there is no failure yet in group 4 and 7, no meaningful 90% statistical confidence ranges for β can be obtained. The 90% statistical confidence ranges for β fitted from all other groups (with failures) actually give us some useful information. For example, group # 5 (11.9W 110°C junction temperature) shows β is close or more than 1 with 90% confidence, suggesting the highest junction temperature group is either at constant failure regime or probably going to wear-out. What's more, β with the lowest upper 90% confidence is ~1.2 and is ~0.85 with the highest lower 90% confidence. If we think failure mode in each group is the same and thus all groups share the same β, Figure 6 indicates β of the whole population is expected to be between 0.85 and 1.2.

Figure 7 depicts the analysis results of comparing the COMD and BCOD failures in the multicell. The time-to-failure and corresponding model at a 10W, 50°C junction use condition are derived using a numerical analysis technique (maximum likelihood estimate) [13]. Shown in the figure are the 90% two-sided confidence ranges of the data from distributions of two failure modes (BCOD and COMD). For the case of BCOD, the obtained 90% statistical confidence ranges for the fitting parameters were $0.3 < \beta < 1.1$, 0.0 eV< Ea <2.3 eV, and $-8.2<n<14.5$. For the case of COMD, the obtained 90% statistical confidence ranges for the fitting parameters were $0.4<\beta<1.4$, 0.4eV<Ea<3.2 eV, and $1.7 < n < 26.3$. Based on the overlapping ranges, we are unable to identify a significant (at the 90% confidence level) difference in the failure statistics of the BCOD and COMD failure mechanism. Similar analysis (not shown here) also indicates no statistically significant (at the 90% confidence level) difference in the failure statistics of the 915 nm and 976 nm groups.

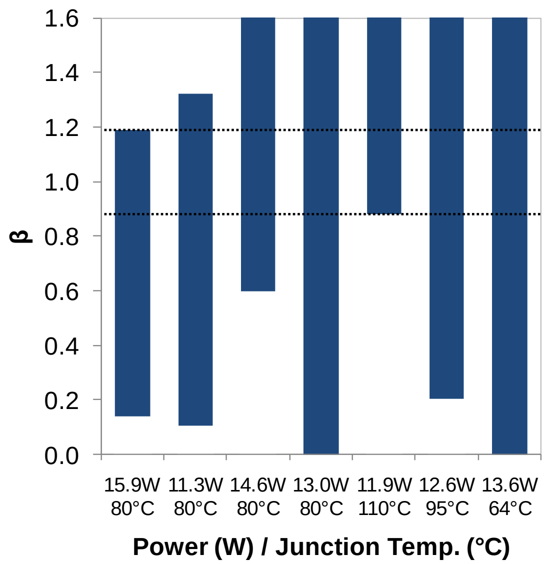

Figure 6: Shape factor β in Weibull distribution for each multi-cell group 1-7 as in Table 1

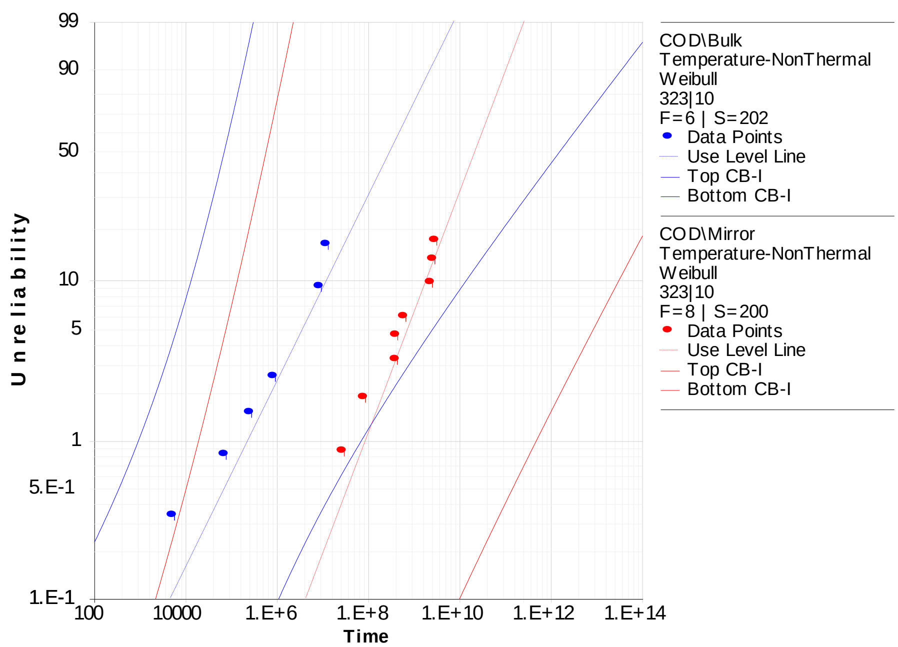

Figure 7: Unreliability vs. time for two failure modes (BCOD and COMD).

Based on the previously discussed analysis of β for each of the 7 multicell groups, the population on the whole is expected to demonstrate β ≈ 1, which corresponding to the exponential or random failure, distribution. In order to better estimate the confidence levels around the extracted acceleration factors and reliability, further analysis is performed making this explicit. Figure 8 depicts the unreliability vs. time for the entire multicell population, fit to the accelerated reliability distribution. Shown in solid lines are the calculated upper and lower 90% two-sided confidence bounds on the distribution.

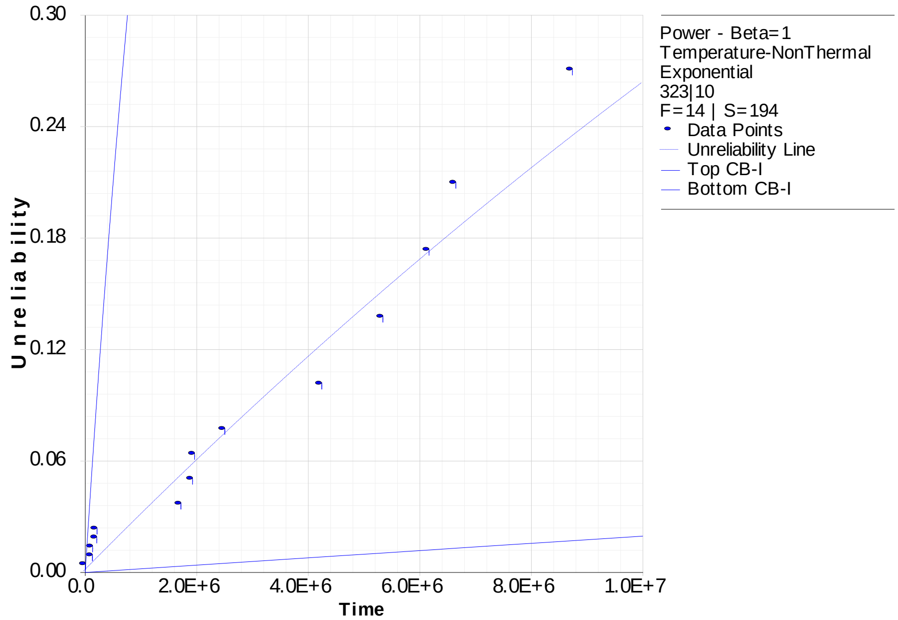

Figure 8: Unreliability vs. time for exponential distribution fitting.

The acceleration parameters for power (n) and temperature (Ea) can be extrapolated from the same fitting with exponential distribution in Figure 8. The results are summarized in Table 3 for various statistical confidence levels (from 50% to 95%). Using parameters in Table 3, the acceleration factors can be calculated for different power/temperature levels, based on equation (1). The results are shown in Figure 9(a) as a function of power at fixed junction temperature, and in Figure 9(b) as a function of temperature at fixed power, separately.

Confidence	n	E_a
95%	> 1.8	> 0.55
90%	> 2.7	> 0.64
80%	> 3.9	> 0.76
70%	> 4.8	> 0.84
60%	> 5.5	> 0.91
50%	> 6.2	> 0.98

Table 3: Acceleration parameters extrapolated with various statistical confidence levels (from 50% to 95%).

Using the 84% single-sided confidence value, the standard deviation around the measured mean values of n and E_a can be calculated. The power acceleration parameter is found to be $n = 6.2 \pm 2.7$ ($\mu \pm \sigma$); the activation energy is $E_a = 0.98 \pm 0.26$ eV ($\mu \pm \sigma$). The FIT score (failure rate in 10^9) at the upper and lower 90% confidence level is found to be 2 < FIT < 470 (the obtained center-line, or 50% confidence value FIT = 30), for the 10W, 25°C heatsink (50°C junction) rated use condition. The Mean Time to Failure (MTTF) is estimated to be >30 years with 90% confidence. The acceleration factors in multi-cell lifetest are also recalculated with the obtained lower-90% (worst-case) values of n and E_a and are shown in Table 4. The 90% lower statistical confidence values of the acceleration factors and reliability at three rated use conditions are shown in Table 5.

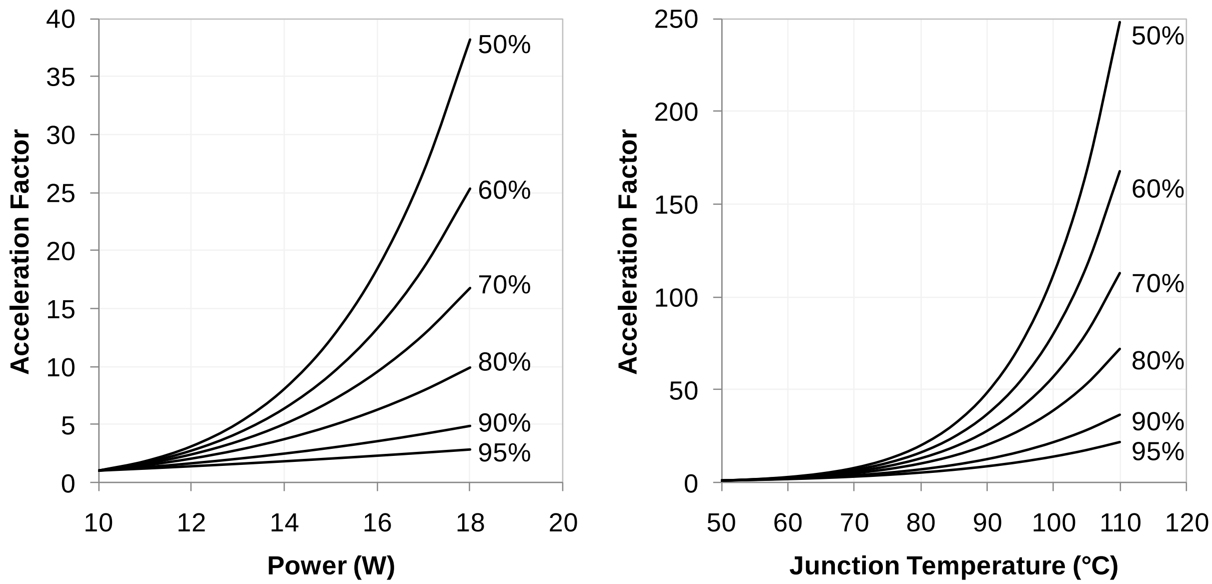

(a) (b)

Figure 9: Acceleration factors calculated for different acceleration levels (a) as a function of power (b) as a function of temperature, (confidence levels from 50% to 95%).

Group	Power (W)	Junction (°C)	$AF_{90\%}$
1	15.9	80	25
2	11.3	80	10
3	14.6	80	20
4	13.0	80	14
5	11.9	110	59
6	12.6	95	31
7	13.6	64	6

Table 4: Acceleration factors in multi-cell lifetest recalculated with extrapolated n/Ea with 90% confidence.

Power (W)	Junction (°C)	$AF_{90\%}$	$B05_{90\%}$ (hours)	$FIT_{90\%}$ (hours)
10	50	1.0	109020	470
12	56	2.5	45330	1132
14	62	5.7	18143	2827

Table 5: 90% lower confidence bound values of the acceleration factor, B05, and FIT score for three rated use conditions.

3. CONCLUSION

In summary, our 915/976 nm diode lasers have demonstrated high performance and high reliability. The high performance and high reliability of these lasers are results of our recent developments on design optimization, facet passivation and manufacturing process control, which are critical to improve performance and reduce COMD and BCOD failures. Multi-cell lifetest of lasers with 3.8mm cavity lengths is being conducted for current up to 18A and junction temperature up to 110°C. They have been running at 12-16W for more than 15000 hours. The acceleration factors and reliability have been extrapolated statistically with 90% confidence bounds specified. The Mean Time to Failure (MTTF) is estimated to be >30 years, for use condition 10W and junction temperature 353K (80°C), with 90% confidence. Multi-cell lifetest data support 9xx nm lasers with 3.8mm cavity lengths be rated to up to 14W, with >95% reliability by 2 years at 70°C (343K) junction. The analysis of multi-cell lifetest data demonstrated high reliability of our high performance 9xx nm diode lasers. On the other side, this is also the main reason for the uncertainties as see in acceleration factor and reliability extrapolations. To get more accurate acceleration factor extrapolations, we need more time to establish enough high failure rates for each acceleration level, which is not very realistic.

REFERENCES

[1] S. Patterson, "Advances in High Power, High Efficiency, High Brightness Fiber Coupled Diode Lasers from 635-nm to 1900-nm and Beyond," 20th Annual Solid State and Diode Laser Technology Review, 2007).

[2] K. Price, S. Patterson, S. Karlsen, A. Brown, R. Mehl, R. Martinsen, K. Kennedy, D. Schutle, and J. Bell, "Progress in Fiber-Coupled, High-Brightness, High-Power Diode Laser Pump Sources," SSDLTR (2008).

[3] K. Price, S. Karlsen, P. Leisher, R. Martinsen, "High Brightness Fiber Coupled Pump Laser Development," Proc. of SPIE, Vol. 7583, 758308 (2010).

[4] L. Bao, J. Wang, M. DeVito, D. Xu, D. Wise, P. Leisher, M. Grimshaw, W. Dong, S. Zhang, K. Price, D. Li, C. Bai, S. Patterson, R. Martinsen, "Reliability of High Performance 9xx-nm Single Emitter Diode Lasers, " Proceedings of SPIE, Vol. 7583, 758302 (2010).

[5] P. Crump, W. Dong, M. Grimshaw, J. Wang, S. Peterson, D. Wise, M. DeFranza, S. Elim, S. Zang, M. Bougher, J. Peterson, S. Das, J. Bell, J. Farmer, M. DeVito and R. Martinsen, "100-W+ Diode Laser Bars Show >71% Power Conversion from 790-nm to 1000-nm and Have Clear Route to > 85%", Proc. of SPIE, Vol. 6456, 645660M (2007).

[6] V. Rossin, E. Zucker, M. Peters, M. Everett and B. Acklin, "High-Power High-Efficiency 910-980nm Broad Area Laser Diodes," Proc. of SPIE, Vol. 5336, 5336-27 (2004).

[7] Z. Yao, E. Zucker, K. Uppal, D. Coblentz, P. Liang, K. Peters, and R. Craig, "High power and high reliability InGaAs broad area lasers emitting between 910 and 980 nm," Lasers and Electro-Optics Society 2000 Annual Meeting. LEOS 2000. 13th Annual Meeting. IEEE, vol. 2, (2000).

[8] T, Strite, "High Reliability Diode Pump Lasers," IEEE SCV LEOS Chapter Meeting, http://www.jdsu.com/products/optical-communications/technology-presentations.html (2007).

[9] Y. Zou, E. Zucker, K. Uppal, D. Coblentz, P. Liang, M. Peters and R. Craig, "Reliability and Performance of InGaAs Broad Area Lasers Emitting Between 910 – 980 nm," Proc. SPIE, Vol. 4285, 159 (2001)

[10] M. Kanskar, M. Nesnidal, S. Meassick, A. Goulakov, E. Stiers, Z. Dai, T. Earles, D. Forbes, D. Hansen, P. Corbett, L. Zhang, T. Goodbough, L. LeClair, N. Holehouse, D. Botez and L.J. Mawst, "Performance and Reliability of ARROW Single Mode & 100μm Laser Diode and the Use of NAM in Al-free Lasers," Proc. of SPIE, Vol. 4995, 196 (2003).

[11] J. Van de Casteele, M. Bettiati, F. Laruelle, V. Cargemel, P. Pagnod-Rossiaux, P. Garabedian, L. Raymond, D. Laffitte, S. Fromy, D. Chambonnet and J. P. Hirtz, "High reliability level on single-mode 980 nm-1060 nm diode lasers for telecommunication and industrial applications", Proc. of SPIE, Vol. 6876, 68760P (2008)

[12] K. Hausler, U. Zeimer, B. Sumpf, G. Erbert and G. Trinkle, "Degradation model analysis of laser diodes," J. Mater Sci: Mater Electron 19, 160 (2008)

[13] ReliaSoft ALTA, http://www.reliasoft.com/alta/index.htm.

[14] Gilly, J.; Friedmann, P.; Kissel, H.; Biesenbach, J.; Kelemen, M. T., "5mm long broad-area lasers at 976nm with 65% efficiency," Proc. SPIE, Vol. 7198, 71980B-7 (2009).

[15] J. Wang, L. Bao, M. Devito, D. Xu, D. Wise, M. Grimshaw, W. Dong, S. Zhang, C. Bai, P. Leisher, D. Li, H. Zhou, S. Patterson, R. Maritinsen and J. Haden, "Reliability and Performance of 808nm Single Emitter Multi-Mode Laser Diodes," Proc. of SPIE, Vol. 7583, 758305, 2010.

[16] L. Bao, J. Wang, M. Devito, D. Xu, M. Grimshaw, W. Dong, P. Leisher, H. Huang, S. Zhang, D. Wise, R. Martinsen, J. Haden, "Performance and Reliability of High Power 7xx nm Laser Diodes," Proc. of SPIE, Photonic West (2011).

[17] Shun-Lien Chuang, N. Nakayama, A. Ishibashi, S. Taniguchi, K. Nakano, "Degradation of II-VI blue-green semiconductor lasers," IEEE J. Quantum Electron., Vol.34, 851 (1998).